

# Numerical Simulation of Recirculation Zone of an Open V-Gutter

C. Lindon Robert Lee<sup>1\*</sup>, A. P. Haran<sup>2</sup>, G. Venkata Krishnan<sup>3</sup> and S. Antony Raja<sup>1</sup>

<sup>1</sup>School of Mechanical Science, Karunya University, Coimbatore - 641114, Tamil Nadu, India; lindonrobertlee@gmail.com, santonyraja@yahoo.co.in

<sup>2</sup>Department of Aeronautical Engineering, Park College of Engineering and Technology, Coimbatore - 641659, Tamil Nadu, India; apharan@rediffmail.com

<sup>3</sup>Linköping University, Sweden; vkgangadharan@live.com

## Abstract

The V-Gutter is a flame stabilizing device used in the afterburners. The flow around this V-Gutter is highly complex due to the recirculating nature of the flow. The flame stabilization is characterised by the length of the recirculation zone hence the determination of recirculation zone is the objective of our study. Since the flow around the gutter is associated with flow separation and recirculation it is sensitive to probe interference and experimentation is costlier hence we resort to numerical simulation. The analysis of flow around the V-Gutter and subsequent determination of the recirculation zone length is carried out with the help of the CFD Software Ansys Fluent. Numerical simulation is carried out for three different included angles of 30°, 45° and 60° but the Blockage is maintained constant from the simulation it is found that the length of the recirculation zone is least for the included angle of 60°. The normalised X/D Values for these angles were 3.520, 3.164 and 2.386 respectively. The increase in blockage from 0.3 to 0.4 increases the recirculation zone length by 33.6%. The findings will be useful for the gas turbine engineers to determine the included angle and the length of the recirculation zone of the V-gutter flame stabilizer.

**Keywords:** Afterburner, Recirculation, V-Gutter

## 1. Introduction

In this paper our objective is to use our high fidelity numerical tool to study the unexplored recirculation length behind the bluff body and find the recirculation length and width. Bluff bodies are used to stabilise the flame for continuous burning in an afterburner of a jet engine. Due to the presence of this bluff body, a very low velocity region exists downstream which helps in anchoring the flame. Since flow separation is a basic phenomenon, numerous experimental studies address this problem of flow separation happening behind a bluff body. There are very few literatures concerning numerical simulation of such phenomena. A specific parameter

has not yet been singled out to be the reason for the flow separation behind a bluff body according to Bradshaw and Wong<sup>1</sup>. Hence, we resort to numerical simulation of flow in a bluff body with various parameters of the bluff body geometry.

Nakanishi et al.<sup>2</sup> conducted experimental investigation on a V-shaped gutter and concluded that this shape compared to others has minimum drag and minimum pressure loss both in burning and Non-Burning condition. Thundil Karuppa Raj et al.<sup>3</sup> conducted an experimental study of recirculating flows and concluded that the recirculation length and width are strongly dependent on the amount of turbulence. From the experimental investigation of M. Sherry et al.<sup>4</sup> on recirculation

\*Author for correspondence

zone formed downstream of a forward facing step, it was found that the re-attachment length tended to increase with Reynolds number for a given  $\delta/h$  ratio, where ‘ $\delta$ ’ is the boundary layer thickness and ‘ $h$ ’ is the step height. According to J. Goodman et al.<sup>5</sup>, the CFD results are very useful in comparing the recirculation length as the exact extent of the reverse flow region could be ascertained only with the help of simulation. As per Kedia K. S. et al.<sup>6</sup>, a bluff body induces favourable conditions for ignition and helps anchoring the flame downstream of the bluff body. Hence, we resort to numerical simulation to determine the recirculation zone length for various V-Gutter configurations.

The textbooks on gas turbine combustion by D. Mattingly<sup>7</sup> and by H. Lefebvre<sup>8</sup> were important materials for the understanding behind the working of afterburners.

The ANSYS Documentation<sup>9</sup> was of immense help behind understanding the usage of ANSYS Tool Fluent.

## 2. Geometric Configuration

The system of interest is to study the behaviour of flow past or over open V-gutter. The V- Gutter used is having a included angle of 30, 45 and 60 degrees which is held in a test section subjected to upstream steady turbulent flow of x velocity  $u = u_\alpha$  (where  $u_\alpha$  is the free stream velocity). The distances of Upstream and Downstream boundaries from the nose of the V-Gutter are fixed as  $L_U = 0.5\text{m}$  and  $L_D = 2.5\text{m}$  respectively. The blockage ratio is 50% ( $D/H = 0.5$ ). The recirculation length is the measurement of the recirculation region in the direction of the flow. The recirculation length is measured from the downstream side of

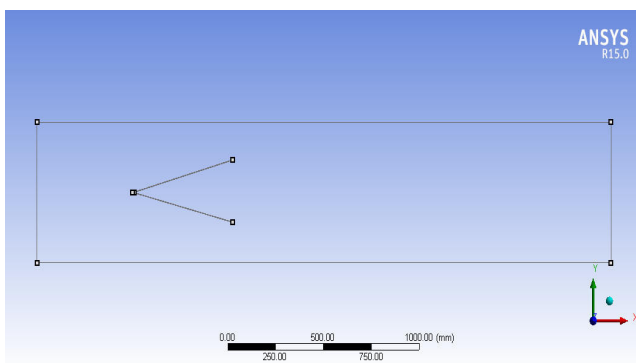


**Figure 1.** Geometric configuration of the computational domain.

the V-Gutter to the point where the X-Velocity changes sign from negative to positive on the line of symmetry.

The system is modelled as a test section with 60cm X 60 cm cross section with 0.5m from inlet to nose of V-Gutter and 2.5m from nose of V-Gutter to exit. A representation is shown in the above Figure 1.

## 3. Boundary Condition

The operating conditions are as tabulated in Table 1.

**Table 1.** Operating Conditions

Bulk Reynolds number $Re_{D_h}$ (calculated from hydraulic diameter $D_h$ )	3,77,595
Inlet velocity $U_{in}$	10 m/s
Inlet temperature $T_{in}$	300 K
Inlet turbulent intensity $T_i$	2%
Inlet pressure $P_{in}$	1 atm
Hydraulic diameter $D_h$	60cm
V-gutter width $D$	30cm
Blockage ratio $B$	0.5

- The left wall of the computational domain is designated as inlet. The velocity inlet boundary condition is assigned as the inlet boundary with free stream velocity  $u = u_\alpha$  and  $v = 0$ .
- The extreme right surface of the computational domain is assigned as outlet. The pressure outlet boundary condition is employed at the exit boundary with zero input value of the static gauge pressure.

## 4. Results and Discussion

From numerical simulations, the data are obtained for geometrical configuration variation of V-Gutter included angle as well as the variation of blockage ratio  $B$ . This results and discussion part focuses on the following three parts:

### 4.1 Comparison of Recirculation Zone Dimensions Obtained by Various Turbulence Models

The recommended turbulence model to be selected for simulating flow around a bluff body is usually K-Epsilon Model. For the purpose of comparison of results,

the data from K-Epsilon Model are compared with data obtained from K-Omega method and Reynolds Stress Model.

The following graphs show the variation of Centre-Line X-Velocity along the length in X-Direction represented as normalised value of X/D for the V-Gutter angles of 30, 45 and 60 degrees obtained by the turbulence models K-Epsilon, K-Omega and Reynolds Stress Model.

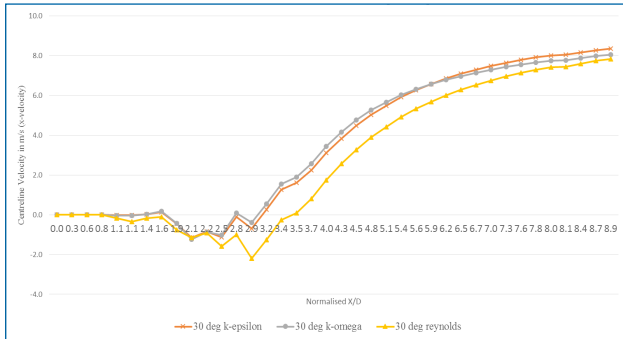


**Figure 2.** Prediction variation between models for 30 degree V-Gutter Angle.

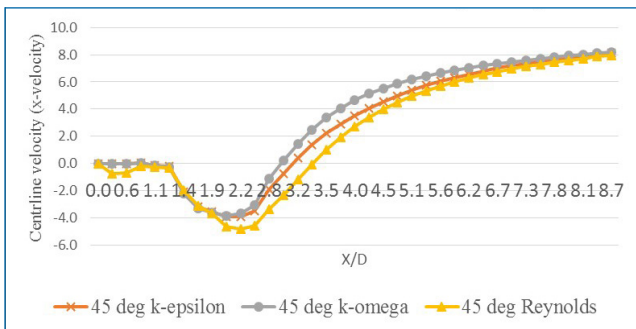


**Figure 3.** Prediction variation between models for 45 degree V-Gutter Angle.

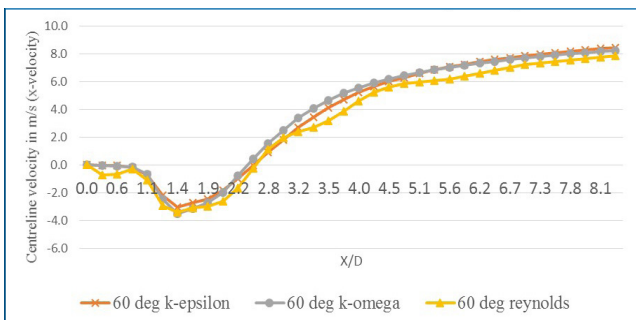


**Figure 4.** Prediction variation between models for 60 degree V-Gutter Angle.

It is observed from the graphs that the K-Epsilon and K-Omega Model are in close agreement which is not the case with results from Reynolds Stress Model.

## 4.2 Effect of Variation of the V-Gutter Angle on the Dimensions of the Recirculation Zone

The following graphs show the variation of the Centre-Line Velocity for various V-Gutter angles by various turbulence models. For the sake of understanding the effect of variation of V-Gutter on X-Velocity, the results obtained from the K-Epsilon Model is discussed further.

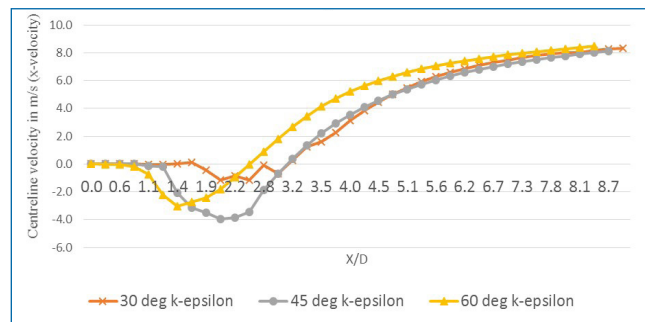


**Figure 5.** K-Epsilon Model Result of centreline X-Velocity vs. X/D for various V-Gutter Angles.

The location along X/D where change of sign in X-Velocity occurs can be taken as an indication of boundary of the recirculation zone. It is observed that compared to other V-Angle configurations, for 60 degree V-Gutter angle, this change in velocity occurs the earliest (at around X/D = 0.8) and also ends the earliest (at around X/D = 2.5).

The highest magnitude of negative X-Velocity occurs for the 45 degree V-Angle configuration, signifying the strongest recirculation zone by x-velocity magnitude. The broadest range of negative X-Velocity occurrence also occurs in this configuration where the sign change of X-Velocity occurs at around X/D = 1.3 and X/D = 3, signifying the start and the end of the recirculation zone respectively.

For the 30 degree configuration, the sign change of X-Velocity starts further higher at X/D value of around 1.5 and ends at around X/D = 2.8. Compared to the other two configurations, the least magnitude of X-Velocity

occurs in this configuration, signifying weak recirculation zone strength by velocity magnitude.

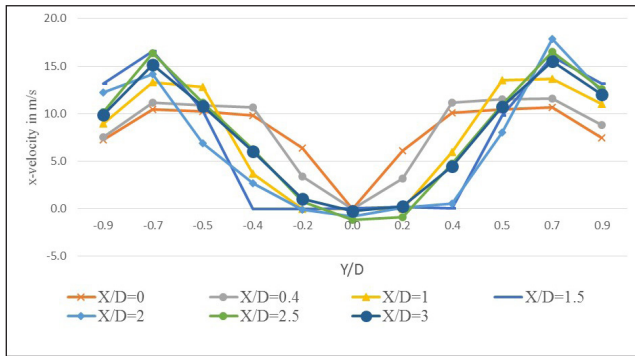


Figure 6. Variation of X-Velocity along Y/D w.r.t. X/D for 30 degree V-Gutter Angle by K-Epsilon Model.

### 4.3 Effect of Variation of Blockage Ratio ‘B’ on the Dimensions of the Recirculation Zone

In the results obtained for the earlier discussions, though the V-Gutter angle was varied, the blockage ratio was maintained a constant by maintaining a constant projected frontal area. However here, to understand the effect of blockage ratio variation on the recirculation zone length, analysis was performed on two configurations differing both in V-Gutter angle as well as the blockage ratio.

The X-Velocity is plotted across the breadth of the V-Gutter represented as a normalised value Y/D. This variation of X-Velocity along Y/D is plotted at various locations along the length in the X-Direction represented as normalised value of X/D. The value Y/D represents centreline of the V-Gutter while positive and negative values of Y/D represent the directions upward and downward from centreline respectively.

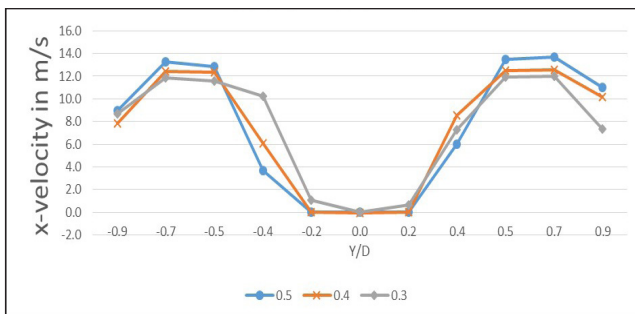


Figure 7. Effect of blockage ratio on variation of X-Velocity w.r.t. Y/D at X/D = 1.

It is observed that the first occurrence of change in sign X-Velocity occurs first for the blockage ratio 0.4 at X/D = 1 followed by blockage ratio 0.5 at X/D = 1.1 and for blockage ratio 0.3 at X/D = 1.5.

The last place where the change in sign of X-Velocity magnitude signifying the end of the recirculation zone occurs the earliest for the blockage ratio B = 0.3 at X/D = 2.2, followed by blockage ratio B = 0.5 at X/D = 3.1 and the farthest along X direction for blockage ratio 0.4 at X/D = 3.25.

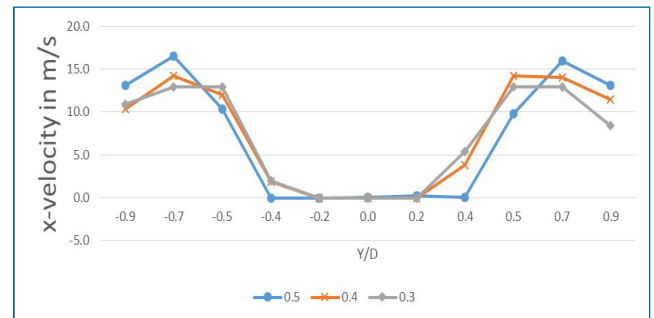


Figure 8. Effect of Blockage Ratio on Variation of X-Velocity w.r.t Y/D at X/D=1.5.

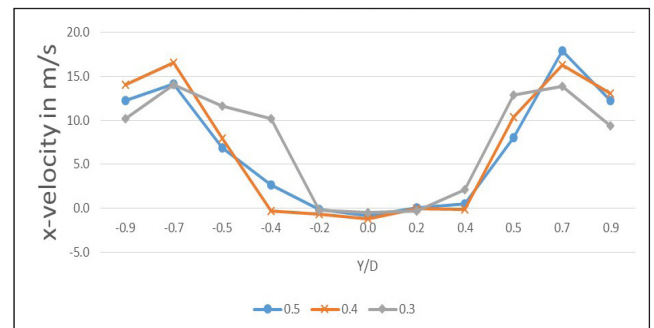


Figure 9. Effect of blockage ratio on variation of X-Velocity w.r.t. Y/D at X/D = 2.

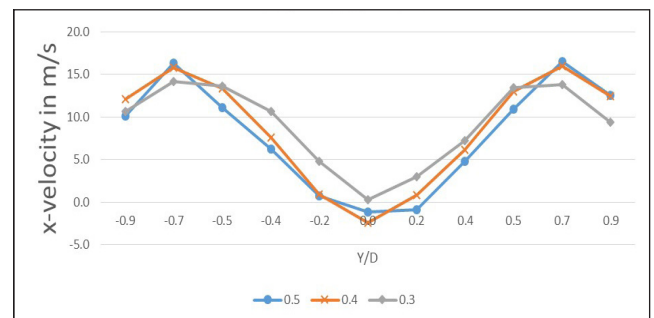
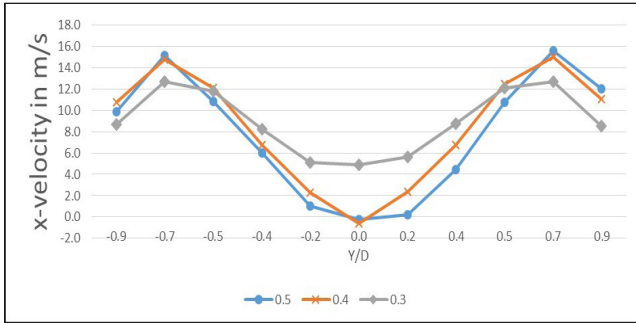


Figure 10. Effect of blockage ratio on variation of X-Velocity w.r.t. Y/D at X/D = 2.5.



**Figure 11.** Effect of blockage ratio on variation of X-Velocity w.r.t. Y/D at X/D = 3.

### 4.4 Recirculation Zone Length

The length of recirculation zone obtained for various V-Gutter angles, various turbulence methods and different blockage ratios are as tabulated below in Table 2.

### 4.5 Grid Independence Study

In the present numerical study three different mesh size (grid 1 = 50,000 and grid 2= 60,000 grid 3 = 70,000) is

**Table 2.** Results consolidation for various configurations of geometry and simulation models

V gutter included angle in degrees	Blockage ratio 'B'	Turbulence Model	Recirculation zone length from nose of V-gutter represented as normalized X/D
30	0.5	k-epsilon	3.109
		k-omega	3.028
		Reynolds Stress	3.520
45	0.5	k-epsilon	2.786
		k-omega	2.557
		Reynolds Stress	3.164
60	0.5	k-epsilon	2.342
		k-omega	2.242
		Reynolds Stress	2.386
18	0.3	k-epsilon	2.377
24	0.4	k-epsilon	3.176
30	0.5	k-epsilon	3.109

adopted. A detailed grid independent study has been performed and results were obtained for the recirculation length but there is no considerable change between grid 2 and grid 3. The grid size of 60,000 is found to meet the requirement of both grid independence and computational time limit. The Figure shows the mean axial velocity downstream of the V-Gutter at various X/D positions for 0.5, 0.6 and 0.7 lakh grids. It is found that the maximum error in axial velocity is less than 4% between 0.6 and 0.7 lakh grid cells. Hence, the grid of 0.6 lakh cells is considered for all further computations.

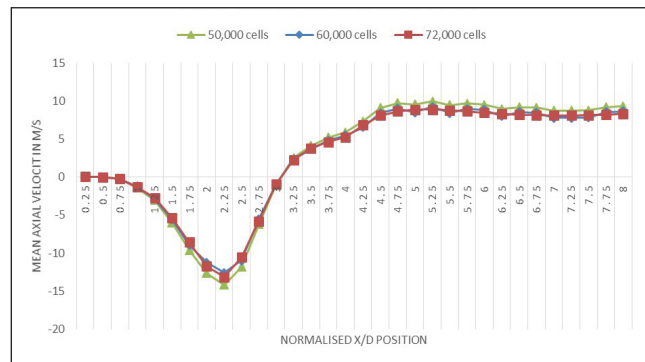


**Figure 12.** Grid Independence Study.

### 4.6 Comparison with Experimental Results

The Experiment was carried out in a wind tunnel with a Test-Section of 3.7m in length and of cross-section 60cm X 60cm. The fan speed was electronically controlled and can be maintained. The V-Gutter was made of SS plate of 3mm thickness. Upstream velocity of 10m/s, 15m/s and 20m/s were utilised to produce a Reynolds number of 0.37x10<sup>6</sup>, 0.4x10<sup>6</sup> and 0.5 X10<sup>6</sup> respectively in the experiments. Velocity was measured downstream of the V-Gutter by means of a Pitot-Static probe which in turn is connected to a water manometer.

$$P_{stag} = \rho_{water} \times g \times h_{stag}$$

$$P_{static} = \rho_{water} \times g \times h_{static}$$

$$P_{stag} = \rho_{static} \times g \times h_{dynamic}$$

$$\rho_{water} \times g \times h_{stag} - \rho_{water} \times g \times h_{static} = \frac{1}{2} \rho_{air} V_{air}^2$$

$$V_{air} = \sqrt{\frac{2\rho_{water} \times g \times (h_{stag} - h_{static})}{\rho_{air}}} \text{ m/s.}$$

Where,

$\rho_{\text{water}}$  is the density of water which is  $1000\text{kg/m}^3$ .

$P_{\text{stag}}$  is the stagnation pressure.

$h_{\text{stag}}$  is the height of water column indicating stagnation pressure.

$P_{\text{static}}$  is the static pressure.

$h_{\text{static}}$  is the height of water column indicating static pressure.

$P_{\text{dynamic}}$  is the dynamic pressure.

$\rho_{\text{air}}$  is the density of air.

$V_{\text{air}}$  is the velocity of air.

$g$  is the acceleration due to gravity.

Thus, we measured the velocity by means of traversing mechanism which is electronically controlled and hence measured the velocity downstream of the bluff body. These experimental results were then compared with numerical simulation only for  $X/D$  value ranging from 3 to 8 since only in this region, positive velocity exists and hence can be measured by experiment. It is found that the experimental results agree with the computational results.

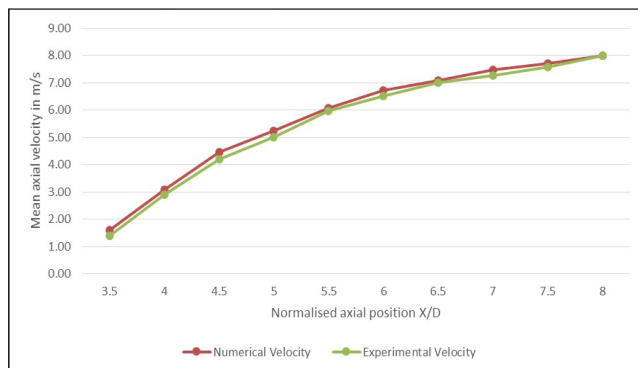


**Figure 13.** Comparison of experimental and numerical data.

## 5. Conclusion

From the numerical results, it can be concluded that results from K-Epsilon and K-Omega models are in close agreement in predicting the velocities very near downstream of the V-Gutter as well as further far away from the V-Gutter than with Reynolds Stress Model.

When the results from same turbulence model are compared, it is inferred that by increasing the included angle of the V-Gutter while maintaining the blockage ratio a constant, the length of the recirculation zone is reduced.

When the V-Gutter angle is increased from 18-degrees to 24-degrees with a corresponding increase of the blockage ratio from 0.3 to 0.4, it is observed that the recirculation zone length increases significantly by around 33.6%. With further increase of V-Gutter angle to 30-degrees with corresponding blockage ratio increase to 0.5, there is a minor drop in the recirculation zone length by around 2.1%.

## 6. Reference

- Bradshaw P, Wong F. The re-attachment and relaxation of a turbulent shear layer. *Journal of Fluid Mechanics*. 1972; 52(1):113–35.
- Nakanishi S, Velie W, Bryant L. An investigation of effects of flame holder gutter shape on afterburner performance. *NACA Research Memorandum, NACA RM E53J14*. 1954.
- Raj TK, Ganesan V. Experimental study of recirculation flows induced by vane swirler. *Indian Journal of Engineering and Materials Sciences*. 2009; 16:2.
- Sherry M, Jacono DL, Sheridan J. An experimental investigation of the recirculation zone formed downstream of a forward facing step. *Journal of Wind Engineering and Industrial Aerodynamics*. 2010; 98(12):888–94.
- Goodman J, Ireland P. Heat transfer and flow investigation of a multi-spoke flame holder for an annular combustor. *Flow, Turbulence and Combustion*. 2008; 81(1-2):261–78.
- Kedia KS, Ghoniem AF. The anchoring mechanism of a bluff-body stabilized laminar premixed flame. *Combustion and Flame*. 2014; 161(9):2327–39.
- Mattingly DJ. *Elements of Gas Turbine Propulsion (First Indian Edition)*. USA: Tata McGraw-Hill; 2005.
- Lefebvre HA, Ballal RD. *Gas Turbine Combustion (First Indian Edition)*. CRC Press; 2013.
- SAS IP Inc. ANSYS Inc. PDF Documentation for Release 15.0. Available from: <http://148.204.81.206/Ansys/readme.html>